Rheol. Acta **12**, 41–47 (1973)

*From the University of Wisconsin-Madison Rheology Research Center (U.S.A.)
and the Mess- und Prüflaboratorium, Badische Anilin & Soda Fabrik, Ludwigshafen am Rhein (Germany)*

Comparison of network theory predictions with stress/time data in shear and elongation for a low-density polyethylene melt

By *A. S. Lodge* and *J. Meissner*

With 7 figures and 2 tables

(Received July 29, 1972)

1. Introduction

An extensive series of rheological measurements has been made on a stabilized low-density polyethylene melt ["Melt I" (1) at 150 °C] having the following properties: density 0.920 g/ml at 20 °C; melt flow index (190/2.16) = 1.33; low-shear-rate viscosity at 150 °C = 5.0×10^5 poise; M_w/M_n = 28.1; M_w = 482,000; CH_3/1000 C = 31. For elongational flow with a step-function elongation rate, *Meissner* (1) has measured tensile stress (as a function of time) and ultimate free recovery. *Chang* and *Lodge* (2) have compared *Meissner*'s stress/time data with the predictions of the network theory "rubberlike liquid" constitutive equations, using a memory function equal to a sum of five exponential terms; the coefficients and exponents ("set A") were chosen to fit the stress/time data at the lowest elongation rate (0.001 sec^{-1}). Subsequently, *Chang* (3) used a second set ("set B") of coefficients and exponents, and obtained a somewhat improved fit of the same data.

In the present paper, we present results of measuring shear stress p_{21} and primary normal stress difference $N_1 = p_{11} - p_{22}$ as functions of time in shear flow with a step-function shear rate of magnitude $\dot{s}$, we compare stress/time data obtained in elongation and shear flows; and we consider whether the network theory gives a better description of the data in elongation than in shear. All data in this paper refer to "Melt I" at 150 °C.

2. Shear flow data

The shear flow data reported here were obtained with a *Weissenberg* Rheogoniometer Model R 12/15 modified, as described by *Meissner* (4), so as to improve the reliability of stress/time data obtained with liquids of viscosity up to 10^6 poise at elevated temperatures. The modifications involved stiffening of the apparatus, replacement of the servo-mechanism by a direct thrust-measurement system, and use of an improved heating system for the specimen under test. The cone-and-plate system was used with the following values of gap angle and gap diameter: 8° and 24 mm for $\dot{s} \geqslant 0.1$ sec^{-1}; 10° and 72 mm for $\dot{s} < 0.1$ sec^{-1}.

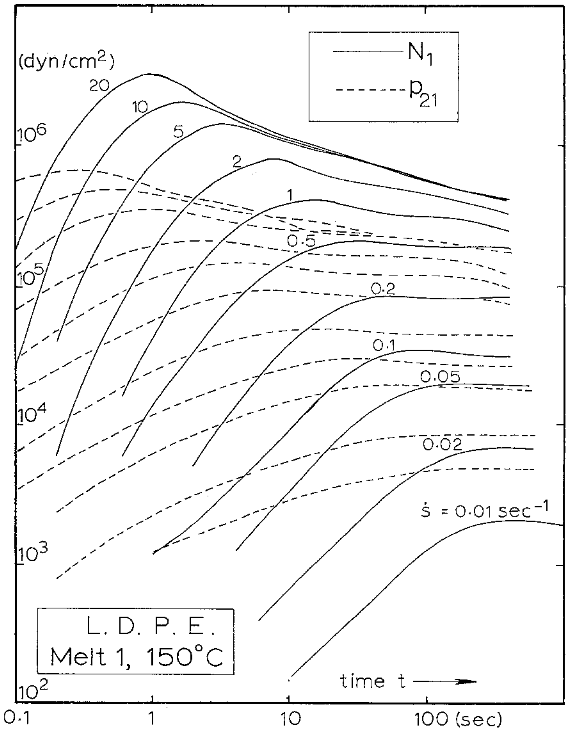

Fig. 1. Measured values of $\log N_1$ and $\log p_{21}$ as functions of $\log t$ for shear flow with step-function shear rate starting at $t = 0$. Shear rate values are given for the N_1 curves; the same shear rate values apply to the p_{21} curves taken in order on the left of the figure

In fig. 1, the data for $\log N_1$ and $\log p_{21}$ as functions of log t are presented for different values of the shear rate $\dot{s}$; the time t is measured from the instant ($t = 0$) at which the shear rate was first applied, the liquid having been at rest for a sufficient period before $t = 0$. It is seen that the familiar maxima are obtained, with the N_1 maxima occurring later than the p_{21} maxima. At the higher shear rates (above 2 sec^{-1}), it is seen that there is a region of values of $\log t$ throughout which N_1 is substantially independent of $\dot{s}$; this behavior is completely different from that at lower shear rates, and is rather unusual. It is intended to make further tests in this region to see, in particular, whether the shear flow is homogeneous throughout the gap. In the present paper, we confine our attention to the lower shear rate region ($\dot{s} \leqslant 2$ sec^{-1}), where the strain rates are comparable with those used in the elongational flow experiments reported previously (1).

The constitutive equations for the "rubberlike liquid" may be written in the form

$$\pi(P,t) + p\gamma^{-1}(P,t) = \int_{t'=-\infty}^{t} \mu(t-t')\,\gamma^{-1}(P,t')\,dt', \qquad [2.1]$$

where $\pi(P,t)$ and $\gamma^{-1}(P,t)$ denote the contravariant body stress and reciprocal metric tensors at particle P and time t; p is a scalar; and the memory function $\mu(t-t')$ is a scalar function of the time interval $t - t'$ (5, 6). Following *Chang* (3), we shall use the following form for μ:

$$\mu(\tau) = \sum_{r=1}^{5} a_r \exp(-\tau/\tau_r) \qquad [2.2]$$

the values of the constants a_r, τ_r ("set B") are given in table 1. Their values have been chosen to make the predictions of [2.1] fit the stress/time data of *Meissner* (1) in elongational flow with a step-function elongation rate $\dot{e}$ of magnitude 0.001 sec^{-1}.

Table 1. Constants ("set B") for the memory function [2.2] for a low-density polyethylene ("Melt I") at 150 °C. These constants have been chosen by *Chang* (3) to fit the measured values of tensile stress as a function of time in elongational flow at an elongation rate $\dot{e} = 0.001$ sec^{-1}

r	τ_r (sec)	a_r (dyn/cm²/sec)
1	10^3	1.6×10^{-3}
2	10^2	1.926×10
3	10	1.723×10^3
4	1	6.64×10^3
5	10^{-1}	3.972×10^5

For a rectilinear shear flow whose velocity components, referred to a rectangular *Cartesian* coordinate system $0x_1x_2x_3$ fixed in space, are $v_1 = \dot{s}x_2$, $v_2 = v_3 = 0$, in which $\dot{s}$ is zero for $t < 0$ and constant for $t \geqslant 0$, it is a straightforward matter to derive from [2.1] the following well-known equations

$$N_1(t) = 2\dot{s}^2 \sum_{r=1}^{5} a_r \tau_r^3 [1 - (1 + t/\tau_r)\exp(-t/\tau_r)], \qquad [2.3]$$

$$p_{21}(t) = \dot{s} \sum_{r=1}^{5} a_r \tau_r^2 ([1 - \exp(-t/\tau_r)]. \qquad [2.4]$$

The curves obtained from these equations, using the "set B" constants of table 1, are shown in figs. 2 and 3 along with the experimental data curves selected from fig. 1.

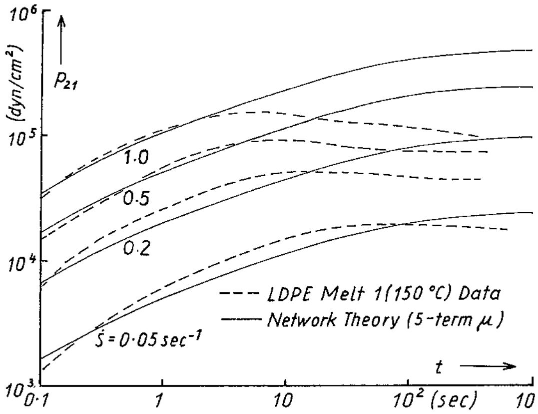

Fig. 2. Comparison of network theory predictions with measured values of shear stress as functions of time from the start of shear flow at constant shear rate $\dot{s}$

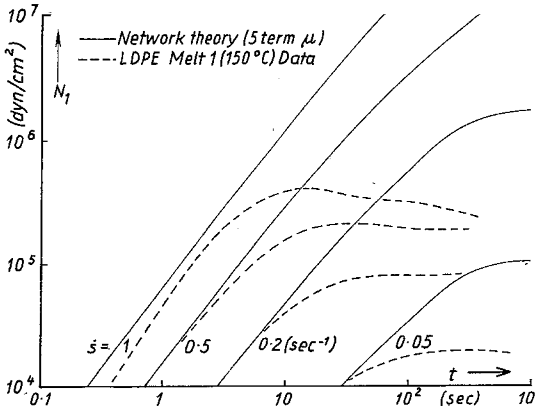

Fig. 3. Comparison of network theory predictions with measured values of primary normal stress difference as functions of time from the start of shear flow at constant shear rate $\dot{s}$

Because the memory function constants were chosen to fit data obtained in a different kind of experiment (elongational flow), with the constitutive eq. [2.1] thereby completely determined for the material in question, the comparison between theory and experiment represented by figs. 2, 3 is a significant test of the network theory. It is seen that the agreement between theory and experiment is good during rather limited time intervals following the start of shear flow; for longer time intervals, there is very substantial disagreement: predicted values of N_1 are as much as 100 times greater than those observed.

In the elongational flow experiments, on the other hand, predicted values for the tensile stress did not exceed the observed values by more than a factor of about 3 [*Chang* (3)]. It appears, therefore, that the network theory description of stress/time behavior in "Melt I" is much worse in shear flow than it is in elongational flow. We think that it would be rather hard to account for such a paradox in molecular terms. However, by examining the comparison of shear flow and elongational flow more closely, we shall show that the paradox disappears, i.e. that the discrepancies between theory and experiment are about equal in size for shear flow and for elongational flow.

3. Comparison of shear flow and elongational flow

As one possible basis for comparing different kinds of flow, it is natural to consider the principal values of the various tensors involved because these can be evaluated in a manner which does not depend on the choice of any special coordinate system such as the coordinate system $0x_1x_2x_3$ used to define N_1 and p_{21} in shear flow. The principal values of stress, strain, and strain rate are given in table 2 in terms of measured quantities for both shear flow and elongational flow [see e.g. (7), pp. 36, 46, 282].

Table 2. Principal strain rates $\varkappa_i$, principal elongation rates $\lambda_i(0, t)$, and principal stresses σ_i for elongational flow and shear flow at constant elongation rate $\dot{\varepsilon}$ and constant shear rate $\dot{s}$. F, A, and p_a denote applied tensile force, cross-sectional area, and ambient pressure in elongation of a cylindrical filament. $\alpha = \varkappa_1 t/2$; $\cot 2\chi' = (p_{11} - p_{22})/(2p_{21})$; $p_{11} > 0$ for a tensile normal component of stress

	Elongation $v_1 = \dot{\varepsilon} x_1$	Shear $v_1 = \dot{s} x_2$
$\varkappa_1$	$2\dot{\varepsilon}$	$\dot{s}$
$\varkappa_2$	$-\dot{\varepsilon}$	$-\dot{s}$
$\varkappa_3$	$-\dot{\varepsilon}$	0
λ_1	e^{α}	$(1 + \alpha^2)^{1/2} + \alpha$
λ_2	$e^{-\alpha/2}$	$(1 + \alpha^2)^{1/2} - \alpha$
λ_3	$e^{-\alpha/2}$	1
σ_1	$F/A - p_a$	$(p_{11} + p_{22})/2 + p_{21} \operatorname{cosec} 2\chi'$
σ_2	$-p_a$	$(p_{11} + p_{22})/2 - p_{21} \operatorname{cosec} 2\chi'$
σ_3	$-p_a$	p_{33}

Table 2 emphasizes the well-known fact that, although the shear flow and elongational flow considered are steady in the sense that their principal strain rates are independent of time, the principal elongation ratios $\lambda_i(0, t)$ depend on time t in ways which differ markedly for shear flow and elongational flow; the greatest principal elongation ratio λ_1 is represented as a function of time in fig. 4.

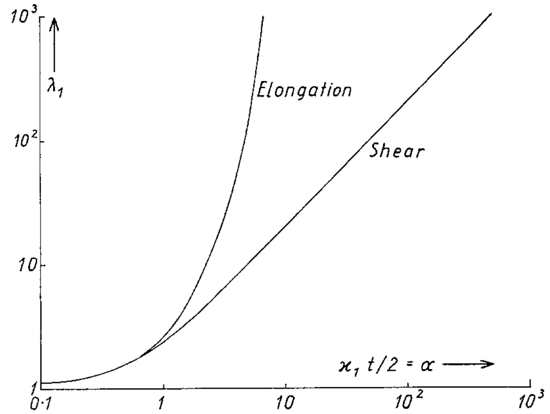

Fig. 4. Comparison of values of the greatest principal elongation ratio $\lambda_1(0, t)$ for elongational flow and shear flow at constant principal elongation rate $\varkappa_1$

To compare the variation of stress with time for shear flow and elongational flow, we shall evaluate the ratio $\Delta p/\Delta\varkappa$, where

$$\Delta p = \sigma_1 - \sigma_2 = \begin{cases} F/A & \text{(elongation)} \\ (N_1^2 + 4p_{21}^2)^{1/2} & \text{(shear)}, \end{cases} \quad [3.1]$$

and

$$\Delta\varkappa = \varkappa_1 - \varkappa_2 = \begin{cases} 3\dot{\varepsilon} & \text{(elongation)} \\ 2\dot{s} & \text{(shear)}. \end{cases} \quad [3.2]$$

This choice of $\Delta p/\Delta\varkappa$ no doubt represents an improvement over the choice of either $p_{21}/\dot{s}$ or $N_1/\dot{s}$, but still involves some arbitrariness: we could also take Δp to equal $\sigma_1 - \sigma_3$ in shear flow. The denominator $\Delta\varkappa$ perhaps also involves some arbitrariness, because the stress and strain-rate tensors have common principal directions in elongational flow but not in shear flow.

For an incompressible *Newton*ian liquid of viscosity η, we have the result that $\Delta p/\Delta \varkappa = \eta$ for shear flow and for elongational flow.

In fig. 5, the values of $\log(\Delta p/\Delta \varkappa)$ obtained from measured stress components are plotted as functions of $\log t$. The shear data are selected from those of fig. 1 above; the elongation data have been published by *Meissner* (1). It is seen that, at the lowest

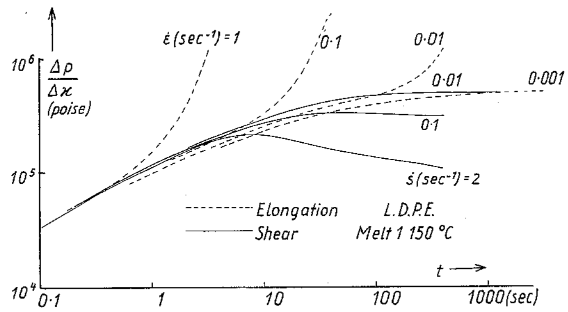

Fig. 5. Comparison of measured values of stress in elongational flow and shear flow. Ordinate: $\log(\Delta p/\Delta \varkappa)$, where Δp and $\Delta \varkappa$ denote differences of principal values of stress and strain rate; abscissa: $\log t$. Numbers near curves denote values of elongation rate $\dot{\varepsilon}$ and shear rate $\dot{s}$

strain rates, shear data and elongation data fall near a common curve; at higher strain rates, data fall near this curve at short times but deviate from this curve at longer times; at the longer times and higher strain rates, shear data and elongation data are very different: the shear data fall below the low-strain-rate curve while the elongation data lie above this curve.

A possible explanation for the observed difference in shear flow and elongation flow at constant principal strain rates is suggested by fig. 4 above, coupled with the elastic recovery data of *Meissner* (1), fig. 7. As the elongation rate is increased, the elastic recovery increases and approaches values appropriate to a perfectly elastic solid. This supports the otherwise plausible suggestion that, for "Melt I" at 150 °C, the stress at time t is more strongly dependent on the total strain measured from $t = 0$ than on the values of principal strain rates at time t; if this is so, then the two types of experiment considered here differ significantly not only in their geometrical aspects but also in the time dependence of their flow histories. For a *Newton*ian liquid, the latter difference would be expected to be unimportant because the extra stress is determined by the current rate-of-strain tensor. It would be of interest to perform a different elongational flow experiment in which the strain was made to vary with time in such a way that the curve for $\lambda_1(0, t)$ coincided with the corresponding curve for shear flow at constant shear rate.

4. Comparison of network theory with experimental data

The predictions of the network theory rubberlike-liquid constitutive equations have been compared with shear flow data in figs. 2 and 3 above and with elongational flow data by *Chang* (3). To see whether the agreement is in fact better for elongational flow than for shear flow, we now seek a method of combining the two comparisons in a single representation.

As a first step, we change the ordinate to the ratio $(\Delta p)_{th.}/(\Delta p)_{ex.}$, where $(\Delta p)_{th.}$ denotes the value of $\sigma_1 - \sigma_2$ calculated from the network theory equations using "set B" constants, and $(\Delta p)_{ex.}$ denotes the value of $\sigma_1 - \sigma_2$ calculated from the experimental data; the same time t is used in numerator and denominator. Agreement between theory and experiment is represented by the value unity for this ratio. In fig. 6,

$$\log[(\Delta p)_{th.}/(\Delta p)_{ex.}]$$

is plotted as a function of $\log t$; the fact that data for different strain rates lie on widely separated curves suggests that the use of a different abscissa might yield a common curve for all the data.

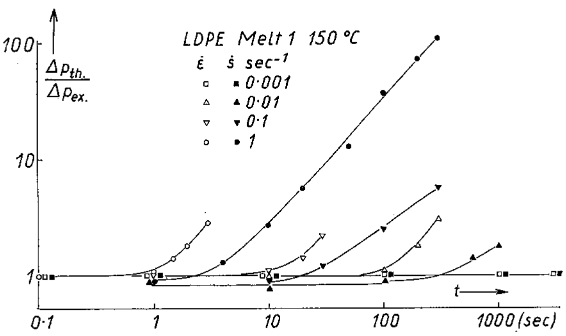

Fig. 6. Comparison of network theory predictions and measured values of stress for elongational and shear flows at constant elongation rates $\dot{\varepsilon}$ and shear rates $\dot{s}$ first applied at $t = 0$. Ordinate: $\log(\Delta p_{th.}/\Delta p_{ex.})$, where $\Delta p_{th.}$ and $\Delta p_{ex.}$ denote values of a difference of principal stresses obtained from theory and from experiment. Abscissa: $\log t$

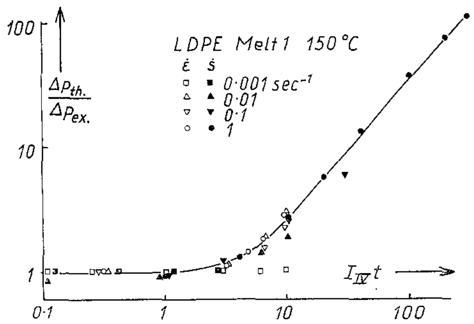

Fig. 7. Comparison of network theory predictions and measured values of stress. Ordinate: as in fig. 6. Abscissa: $\log(I_{\text{IV}}t)$, where I_{IV} is the rate-of-strain invariant defined in [4.1]

As a result of a somewhat haphazard procedure, in which various symmetric functions of the principal strain rates $\varkappa_i$ were tried, we have found that most of the data points fall near a common curve (fig. 7) when $I_{\text{IV}}\, t$ is used as abscissa, where

$$I_{\text{IV}} = 2^{-1/2} \Big\{ \Big(\sum_{i=1}^{3} \varkappa_i^2 \Big)^{1/2} + \Big| \sum_{i=1}^{3} \varkappa_i^3 \Big|^{1/3} \Big\} \qquad [4.1]$$

$$= \begin{cases} 3.01\, \dot\varepsilon & \text{(elongation)} \\ \dot s & \text{(shear)}. \end{cases} \qquad [4.2]$$

In view of our remarks towards the end of § 3, it is perhaps surprising that we should employ a rate-of-strain invariant I_{IV} (rather than a strain invariant, for example) in this context. We do not claim that the use of $I_{\text{IV}}\, t$ as abscissa furnishes the only (or even the best) way of plotting shear and elongation data so that they fall near a common curve. Two other choices have been made: using $\varkappa_1 t$ and $\lambda_1(0, t)$ as abscissae, we find that the data points lie somewhat further from a common curve than they do in fig. 7.

We make the following comments on fig. 7.

1. The two points furthest from the common curve represent elongation data taken at the lowest elongation rate

$$(\dot\varepsilon = 0.001 \text{ sec}^{-1})$$

and theoretical values obtained under conditions in which theory was made to agree with experiment (by choice of constants in the memory function). It is therefore not unreasonable to find such points lying away from the common curve.

2. The elongation experiments were all subject to the restriction $I_{\text{IV}}\, t \leqslant 10$. In the shear experiments, values of $I_{\text{IV}}\, t$ up to 130 were used. When $I_{\text{IV}}\, t > 10$ in the elongation experiments, the filament becomes so thin that tension measurements are too inaccurate. There is no corresponding restriction in the shear experiments; the use of a rotational apparatus to generate shear flow enables one to measure torque and thrust without limit on the value of $I_{\text{IV}}\, t$, provided that I_{IV} is not so large that the liquid in the cone/plate gap breaks up.

3. The fact that the shear points and most of the elongation points in fig. 7 lie close to a common curve enables us to resolve the paradox stated in § 2 above: *the extent of agreement between the network theory and the experimental data for Melt I at 150 °C is substantially the same for shear flow and for elongational flow*; the fact that, at first sight, the agreement is better for elongational flow can now be attributed to the smaller range of values of $I_{\text{IV}}\, t$ used in elongational flow.

5. Utility of the network theory

The network theory is based on a plausible molecular model for polymeric liquids and gives a qualitatively successful description of some of their main characteristic rheological properties; the prediction that viscosity is independent of shear rate, however, restricts the possible range of validity of the theory, when applied to prolonged flow at constant strain rate, to the region of low strain rates. Hitherto, this has been regarded as a rather severe limitation on the usefulness of the theory.

The results of fig. 7 above suggest, however, that *the network theory may be quantitatively useful for flows of short duration which start from a state in which the liquid has been undeformed for a sufficient length of time.* Fig. 7 shows that, for Melt I at 150 °C, theory agrees with experiment to within about 10% provided that

$$I_{\text{IV}}\, t \leqslant 3. \qquad [5.1]$$

This applies to shear and elongational flows at strain rates which are large enough for the viscosity to vary appreciably with change of shear rate; the measurement of viscosity requires prolonged flow (with $I_{\text{IV}}\, t \gg 3$) at constant shear rate in order that the shear stress shall reach a constant value.

The foregoing conclusions have been based on the results of experiments which use step-function strain rates. It is tempting to speculate that the network theory might also apply to short-duration flows even when the strain rates vary with time, provided, of course, that the flows start from a state of rest. One obvious generalization of the condition [5.1], which might be applicable in such circumstances, is the following:

$$\int_{t'=0}^{t} I_{IV}[\varkappa_i(t')]\,dt' \leqslant 3. \qquad [5.2]$$

It is possible that such considerations could encompass the fact that the network theory has been successfully applied to certain recent experiments. For example, *Astarita* and *Nicodemo* (8) have conducted an experiment in which a free stream of liquid (a solution containing 0.5% Separan ET597 in glycerol) was drawn upwards from a reservoir of liquid at rest; measurements of tensile force and stream profile were found to be consistent with the predictions of the rubberlike-liquid equations with a single-exponential memory function. This experiment involved heterogeneous flow with strain rates which, for a given material element, varied with time. A rough estimate made from the data of figs. 3 and 5 of (8) (taking $\dot{\varepsilon} = du/dx$) yields a value between 1 and 1.5 for the integral in [5.2]. Provided that the same number 3 on the right-hand side of [5.2] is appropriate for the Separan/glycerol solution, it follows that the result of *Astarita* and *Nicodemo* is compatible with the conclusion of the present paper.

The network theory predicts that the viscosity will be independent of shear rate; it is well known that this prediction is associated with the assumptions that junction creation and loss rates are independent of the flow history. Various semi-empirical, semi-molecular, methods of modifying the constitutive equations have been used (9, 10) in order to improve the quantitative utility of the theory. The result [5.2] of the present paper gives some support to those methods of modifying the constitutive equations which permit the memory function to depend on values of rate-of-strain invariants. Even with modifications of this kind, there is a wide choice of possible modifications to be considered; it would be helpful if suitable experiments could be devised to serve as a guide to the "correct" modification to be made for a given polymeric liquid. We have recently proposed (11) the use of rapid, incremental strain, tests for this purpose. It might also be helpful to seek the explanation, in terms of molecular structure, underlying the value 3 for the right-hand side of [5.1] or [5.2].

Acknowledgements

We gratefully acknowledge financial support from the National Science Foundation (Grant No. GK-15611 to A. S. L.) and from the Brittingham Funds (University of Wisconsin-Madison). The experiments were performed in the Mess- und Prüflaboratorium of Badische Anilin- und Soda-Fabrik, Ludwigshafen/Rhein, Germany. We acknowledge the help of Mr. *Hui Chang* in computation and in furnishing memory-function constants. Parts of this paper were presented at the American Physical Society (Division of High Polymer Physics) meeting in April, 1972, and at the Sixth International Congress on Rheology in September, 1972.

Summary

Experimental data are presented which show the variation with time of the shear stress and primary normal stress difference during shear flow with a step-function shear rate; the material ("Melt I" at 150 °C) is a low-density polyethylene melt for which stress-growth and elastic recovery data in elongational flow experiments have been previously reported. A method of comparing the data with the predictions of the rubber-like-liquid constitutive equations is given, based on the use of a specially-chosen rate-of-strain invariant I_{IV}, defined in [4.1]. From this comparison, it is shown that the disagreement between theory and experiment is about the same for shear flow and for elongational flow, and that the extent of disagreement does not exceed 10% for short-duration flows such that

$$I_{IV} t \leqslant 3.$$

Zusammenfassung

Es werden Meßergebnisse über die zeitliche Änderung der Schubspannung und der ersten Normalspannungsdifferenz bei Scherfließen einer LDPE-Schmelze („Schmelze I" bei 150 °C) vorgelegt. Der zeitliche Spannungsverlauf bei und die elastische Erholung nach Dehnfließen sind für dieses Material bereits früher mitgeteilt worden. Hier wird das Verhalten der Schmelze bei Scherung und bei Dehnung mit den Voraussagen der „rubberlike liquid"-Zustandsgleichung verglichen, wobei eine speziell gewählte Invariante I_{IV} der Deformationsgeschwindigkeit verwendet wird (definiert in [4.1]). Der Vergleich zeigt Abweichungen von Theorie und Experiment, die für Scher- und Dehnfließen etwa gleich groß sind. Die Abweichungen liegen unter 10%, wenn für das Produkt aus I_{IV} und der Deformationszeit t der Wert $I_{IV} t = 3$ nicht überschritten wird.

References

1) *Meißner, J.*, Rheol. Acta **10**, 230 (1971).
2) *Chang, Hui* and *A. S. Lodge*, Rheol. Acta **11**, 127 (1972).
3) *Chang, Hui* (to be submitted to Rheol. Acta).
4) *Meissner, J.*, J. Appl. Polymer Sci. **16**, 2877 (1972).
5) *Lodge, A. S.*, Rheol. Acta **7**, 379 (1968).

6) *Lodge, A. S.*, Rheol. Acta **11**, 106 (1972); also University of Wisconsin Mathematics Research Center Technical Service Report 1092.

7) *Lodge, A. S.*, Elastic Liquids (London and New York 1964).

8) *Astarita, G.* and *L. Nicodemo*, Chem. Eng. J. **1**, 57 (1970).

9) *Yamamoto, M.*, Trans. Soc. Rheol. **15** (2), 331 (1971).

10) *Carreau, P. J.*, Trans. Soc. Rheol. **16** (1), 99 (1972).

11) *Lodge, A. S.* and *J. Meissner*, Rheol. Acta **11**, 351 (1972).

Authors' addresses:

Professor *A. S. Lodge*
U. W. Rheology Research Center
1500 Johnson Drive
Madison
Wisconsin 53706
(U.S.A.)

Dr. *J. Meissner*
Mess- und Prüflaboratorium
Badische Anilin und Soda Fabrik A.G.
6700 Ludwigshafen am Rhein
(Germany)